# Research on structure of $Cu_2ZnSn(S, Se)_4$ thin films with high Sn-related phases*

**LI Peng-yu** (李鹏宇)[1], **XUE Yu-ming** (薛玉明)[1]**, **LIU Hao** (刘浩)[1,2], **XIA Dan** (夏丹)[1], **SONG Dian-you** (宋殿友)[1], **FENG Shao-jun** (冯少君)[1], **SUN Hai-tao** (孙海涛)[1], **YU Bing-bing** (俞兵兵)[1,2], and **QIAO Zai-xiang** (乔在祥)[2]

*1. Tianjin Key Laboratory of Film Electronic & Communication Devices, School of Electronics Information Engineering, Tianjin University of Technology, Tianjin 300384, China*

*2. Tianjin Institute of Power Sources, Tianjin 300384, China*

(Received 12 March 2016; Revised 5 October 2016)



$Cu_2ZnSn(S, Se)_4$ (CZTSSe) thin films were deposited on flexible substrates by three evaporation processes at high temperature. The chemical compositions, microstructures and crystal phases of the CZTSSe thin films were respectively characterized by inductively coupled plasma optical emission spectrometer (ICP-OES), scanning electron microscopy (SEM), X-ray diffraction (XRD) and Raman scattering spectrum. The results show that the single-step evaporation method at high temperature yields CZTSSe thin films with nearly pure phase and high Sn-related phases. The elemental ratios of Cu/(Zn+Sn)=1.00 and Zn/Sn=1.03 are close to the characteristics of stoichiometric CZTSSe. There is the smooth and uniform crystalline at the surface and large grain size at the cross section for the films, and no other phases exist in the film by XRD and Raman shift measurement. The films are no more with the Sn-related phase deficiency.

**Document code:** A **Article ID:** 1673-1905(2016)06-0446-4

**DOI** 10.1007/s11801-016-6055-9

$Cu_2ZnSnS_4$ (CZTS, or $Cu_2ZnSn(S, Se)_4$ (CZTSSe)) is one of the promising materials for absorber in thin film solar cell because of its excellent material properties. It has a direct bandgap of around 1.45 eV, which is very close to the optimum value of semiconductor used for photovoltaic solar energy conversion. It exhibits p-type conductivity and high absorption coefficient of $\alpha > 10^4$ $cm^{-1}$. In addition, its constituent elements are more earth-abundant and low toxic[1]. At present, CZTS, CZTSe and CZTSSe solar cells with laboratory efficiencies of 8.4%, 9.7% and 12.6% have been reported respectively[1,2]. Thermal evaporation is still attractive for high efficiency. Up to now, the highest conversion efficiency of CZTSe solar cell is 9.15% by co-evaporation method[3]. CZTS-based films were mostly prepared by evaporation processes which were low-temperature co-evaporation followed by a short/long annealing[4]. CZTS thin film is easy to decompose at a certain temperature. This decomposition reaction will lead to the secondary phase formation, such as CuxS and ZnS. Furthermore, there are easy volatile elements in the CZTSe or CZTSSe thin films, such as Sn. During the fabrication, if the Sn secondary evaporation happens in the films and can not be timely supplied, the films will be lack of Sn, leading to the secondary phases and not able to grow stoichiometric CZTS (or CZTSSe) thin films, which can degrade the CZTS (or CZTSSe) device performances[5-8]. The main problem is the Sn-related phase deficiency for stoichiometric CZTSSe absorber layers by evaporation process. SnS sublimes at 350 °C, SnSe evaporates at 370 °C, and Sn evaporates at 460 °C[9,10].

In this paper, we deposited the CZTSSe absorbers by evaporation process. In order to deposit CZTSSe thin films with desired composition, we made a series of optimization processes and fabricated CZTSSe thin films by single-step evaporation method on flexible substrate at high temperature. The performances of the CZTSSe thin films were characterized to investigate their chemical composition, morphology and crystal structure.

The CZTSSe thin films were fabricated in a vacuum chamber with four evaporation sources. The background pressure of the vacuum chamber is around $1\times10^{-4}$ Pa. The polymide (PI) substrates are 10 cm×10 cm, which were coated with a 1-μm-thick sputtered molybdenum (Mo) back contact. The evaporation sources are copper (Cu), zinc sulfide (ZnS), tin (Sn) and selenium (Se), and their temperatures were controlled by PID temperature controllers. The temperature stability is within ±0.1 °C. The

* This work has been supported by the National High Technology Research and Development Program of China (No.2012AA050701), and the Innovation and Entrepreneurship Training Program for College Students in Tianjin (No.201410060036).

** E-mail: orwell.x@163.com

substrate was rotated to obtain uniform thin film. The CZTSSe thin films were deposited by three types of deposition processes. For Type I, the substrate temperature was set to constant (300 °C). Cu, ZnS, Sn and Se were co-evaporated at low temperature. For Type II, the absorber deposition was performed by a two-stage process: In the first stage, the substrate temperatures of Cu, ZnS, Sn and Se were co-evaporated at 300 °C; In the second stage, the substrate temperature was elevated to 480 °C, then the Cu and ZnS flux was turned off. The deposition was performed in Sn and Se atmosphere to improve crystallinity and compensate for Sn-related phase deficiency. For type III process, the substrate temperature was set to a constant of 480 °C. In the first stage, we co-evaporated the four sources. In the second stage, the Cu and ZnS flux was turned off, and the deposition was performed in Sn and Se atmosphere to compensate for Sn-related phase deficiency.

The chemical compositions of CZTSSe thin films were measured by inductively coupled plasma optical emission spectroscopy (ICP-OES). The surface morphology of the thin films was observed by scanning electron microscope (SEM). The crystal orientation, structures and crystallinity were examined by X-ray diffraction (XRD) analysis using Cu $K_\alpha$ radiation. The films were also analyzed by Raman scattering system with the laser wavelength of 514.5 nm at room temperature.

Tab.1 shows the five elemental compositions and their ratios in CZTSSe thin films. Firstly, the substrate temperature was set at 300 °C, aiming to adjust the chemical composition.

**Tab.1 The elemental compositions and ratios in CZTSSe thin films**

| Sample | Elemental composition (atomic percentage/%) | | | | | Elemental ratio | |
|---|---|---|---|---|---|---|---|
| | Cu | Zn | Sn | S | Se | Cu/(Zn+Sn) | Zn/Sn |
| S1 | 18.19 | 12.64 | 16.62 | 3.26 | 49.29 | 0.62 | 0.76 |
| S2 | 22.72 | 13.41 | 13.05 | 2.27 | 48.55 | 0.86 | 1.03 |
| S3 | 21.46 | 14.31 | 3.71 | 17.42 | 42.90 | 1.20 | 3.86 |
| S4 | 26.25 | 10.18 | 12.63 | 2.58 | 48.35 | 1.15 | 0.81 |
| S5 | 24.79 | 10.94 | 12.57 | 1.95 | 49.75 | 1.05 | 0.87 |
| S6 | 26.16 | 13.61 | 12.55 | 2.09 | 45.59 | 1.00 | 1.08 |

From the elemental ratios of Cu/(Zn+Sn) and Zn/Sn of S1, we can determine the evaporation temperature of four sources. Fig.1 shows the surface and cross section morphologies of CZTSSe thin films. Fig.1(a) and (b) are the flocculent morphologies at the surface and in the cross section, respectively. The crystallinity is bad. Then we used the Type II process. By comparing with samples S2 and S3, when we prolonged the evaporation time of the second stage from 15 min to 30 min, we find that the ratios of Cu/(Zn+Sn) and Zn/Sn increase, and the samples become slightly Cu-rich and obviously Zn-rich. The samples become Zn-rich because of the loss of large amount of Sn, the films were not well synthesized at low temperature, and Sn-related phases exist in the films. With gradual increase of substrate temperature in the second stage, the Sn-related phases disappeared. If the substrate temperature was set to be high at the beginning, the films could be synthesized well, and the loss of Sn-related phases may be reduced. Fig.1(c) and (d) show the very small grain sizes at the surface and layered structure in the cross section. The thicknesses of the films are about 2 μm and the large grains are near the substrates. Then, the evaporation time of the second stage is prolonged, the grains become bigger and the shape is flaky at the surface as shown in Fig.1(e). In Fig.1(f), the layered structure still exists, but the large grains are near the surfaces and the substrates. Considering the chemical composition and morphology of Type II process, we select the Type III process finally. The ratios of Cu/(Zn+Sn) and Zn/Sn are respectively 1.15 and 0.81, which indicate that the films are Cu-rich and Zn-poor. From Fig.1(g) and (h), there are large grains with average size of 0.6—1 μm in the CZTSSe thin films, and the grains are columnar and throughout the films. Furthermore, after adjusting the ZnS evaporation temperature, the sample S6 becomes better, and the ratios of Cu/(Zn+Sn) and Zn/Sn are close to those of the stoichiometric CZTSSe films. The films are no longer the Sn-related phase deficiency. From Fig.1(i)—(l), the small piece grains are less than those of sample S4, and sample S6 is smooth and uniform at the surface and has large grains in the cross section.

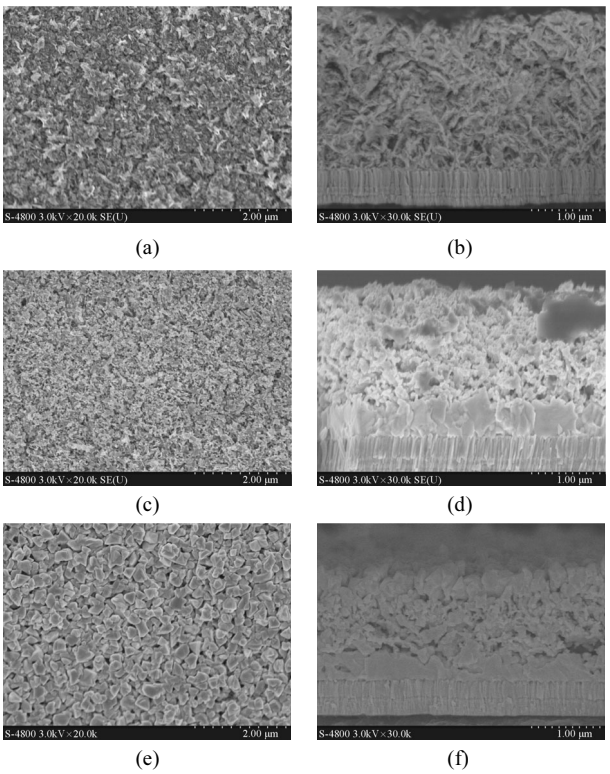


(a) (b) (c) (d) (e) (f)

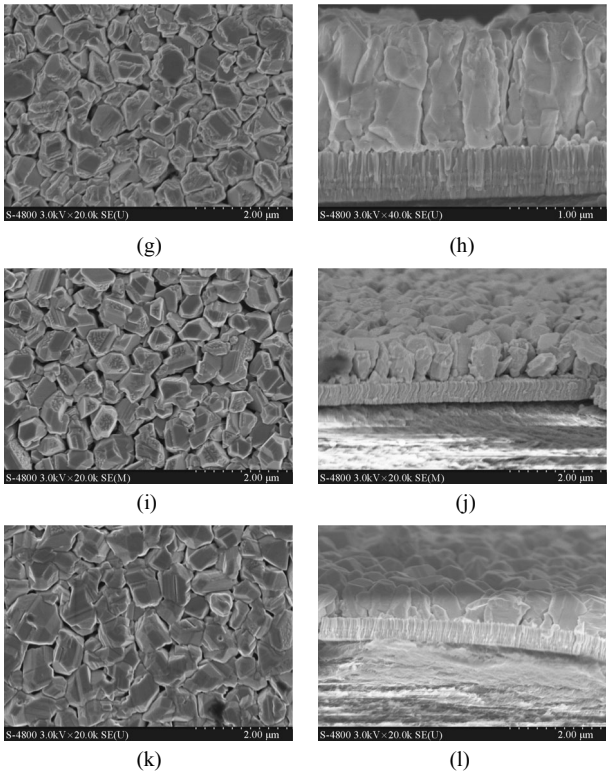


**Fig.1 The surface (left) and cross-section (right) SEM images of the CZTSSe thin films**

Fig.2 shows the XRD patterns of CZTSSe thin films deposited by different processes. There are the main $Cu_2ZnSnSe_4$ diffraction peaks at 27.4°, 45.4° and 53.8°. This results are in good agreement with other reports[11, 12].

Fig.3 shows the full width at half maximum (*FWHM*) values of (112), (220)/(204) and (312)/(116) diffraction peaks of the CZTSSe films. As shown, the samples S4, S5 and S6 deposited by Type III process have better crystalline due to the low *FWHM*. Generally, ZnSe (PDF card No.37-1463) and $Cu_2ZnSe_3$ (PDF card No.65-7524) have similar symmetry and lattice parameters with CZTSe, and the main diffraction peaks of these phases overlap. So Raman spectra are required to recognize these phases. Fig.4 shows the Raman spectra of different samples. For sample S6, the main peaks of the CZTSe films are at 172—173 $cm^{-1}$, 194—197 $cm^{-1}$, 231—235 $cm^{-1}$

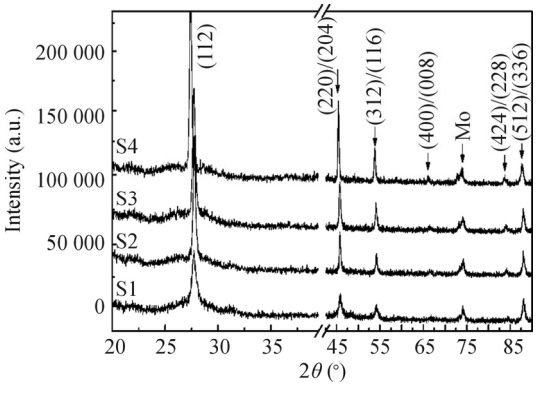


(a) Samples S1—S4

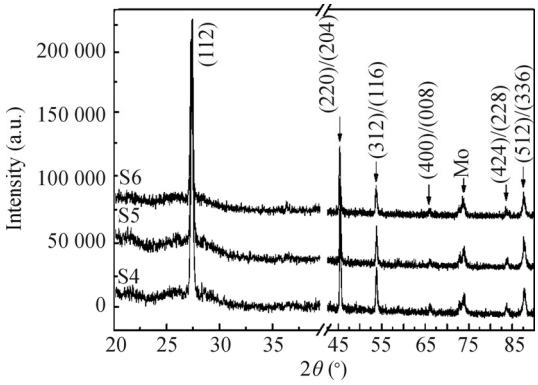


(b) Samples S4—S6

**Fig.2 XRD patterns of CZTSSe thin films deposited by different processes**

and 239—254 $cm^{-1}$[11,12]. For sample S1, the CZTSe main peaks are at 190 $cm^{-1}$ and 195 $cm^{-1}$ (the same as XRD data). There are ZnSe[13] peaks for samples S1 and S3 at 251 $cm^{-1}$. For sample S4, there is $SnSe_2$[14] peak at 182 $cm^{-1}$ and $Cu_{2-x}Se$[15] peak at 256 $cm^{-1}$. There are $Cu_2SnSe_3$[16] peaks for samples S3 and S5 at 180 $cm^{-1}$. For sample S2, there is ZnS[17] peak at 350 $cm^{-1}$. In short, there are pure CZTSe phases in sample S6.

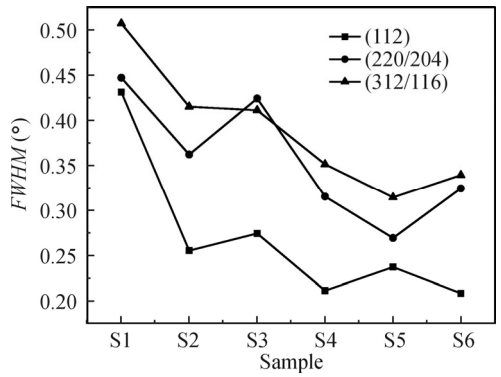


**Fig.3 *FWHM* values of (112), (220)/(204) and (312)/(116) diffraction peaks of the CZTSSe**

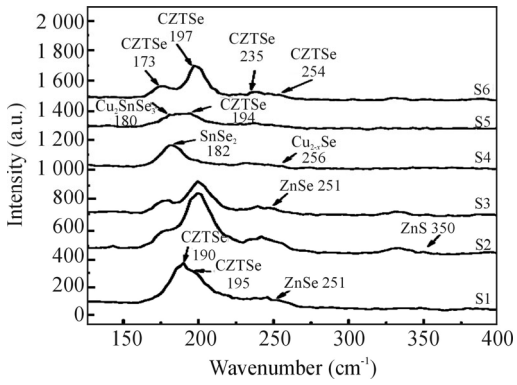


**Fig.4 Raman spectra of CZTSSe thin films**

The reaction mechanism to form quaternary CZTSe compounds has been studied[14], which can explain the

formation of different phases in the CZTSe thin films. For sample S3, the ratios of Cu/(Zn+Sn) and Zn/Sn are respectively 1.2 and 3.86, which make the excessive ZnSe react with $Cu_2SnSe_3$ to form $Cu_2ZnSnSe_4$, so sample S3 shows the phase of ZnSe. For sample S4, the substrate temperature is a constant (480 °C), and the excessive Sn and Se formed $SnSe_2$. So sample S4 shows the phase of $SnSe_2$. For sample S5, the ratios of Cu/(Zn+Sn) and Zn/Sn are respectively 1.05 and 0.87, where there is no enough ZnSe to react with $Cu_2SnSe_3$ and form CZTSe, so sample S5 shows the phase of $Cu_2SnSe_3$. The Cu/(Zn+Sn) values are respectively 1.20, 1.15 and 1.05 for samples S3, S4 and S5, which show excessive copper in the films to form $Cu_{2-x}Se$. However, for sample S6, the values of Cu/(Zn+Sn)=1.00 and Zn/Sn=1.03 are close to those of the stoichiometric CZTSSe, and it is pure because of no redundant copper and zinc to form other phases.

An effective synthesis process was successfully employed to fabricate CZTSSe thin films by single-step evaporation method on flexible substrate at high temperature, and the deposition processes of CZTSSe absorber layers were optimized. The CZTSSe thin films (the same as sample S6) deposited by the optimized process are good stoichiometric CZTSSe thin films, they are very smooth and uniform at the surface and have large size grains. No other phases exist in the thin films. The thin films are no more with the Sn-related phase deficiency.

## References

[1] T.S. Shyju, S. Anandhi and R. Suriakarthick, Journal of Solid State Chemistry **227**, 165 (2015).

[2] Shin B, Gunawan O and Zhu Y, Progress in Photovoltaics Research & Applications **21**, 72 (2013).

[3] Repins, Ingrid and Beall, Solar Energy Materials & Solar Cells **101**, 154 (2012).

[4] Wang K, Gunawan O and Todorov T, Appl. Phys. Lett. **97**, 143508 (2010).

[5] Swati J. Patil, Vaibhav C. Lokhande and Dong-Weon Lee, Optical Materials **58**, 418 (2016).

[6] Weber A, Mainz R and Schock H W, J. Appl. Phys. **107**, 013516 (2010).

[7] Redinger A and Siebentritt S, Appl. Phys. Lett. **97**, 092111 (2010).

[8] Redinger A, Berg D M, Dale P J and Siebentritt S, J. Am. Chem. Soc. **133**, 3320 (2011).

[9] Matsushita H, Maeda T and Katsui A, Journal of Crystal Growth **208**, 416 (2000).

[10] Jing Guo, Wen-Hui Zhou and Ying-Li Pei, Solar Energy Materials & Solar Cells **155**, 209 (2016).

[11] Salomé PMP, Fernandes PA and da Cunha AF, Thin Solid Films **517**, 2531 (2009).

[12] Ahn S, Jung S and Gwak J, Appl. Phys. Lett. **97**, 021905 (2010).

[13] Amiri N B M and Postnikov A, Phys Rev B **82**, 1616 (2010).

[14] Ennaoui A, Lux-Steiner M and Weber A, Thin Solid Films **517**, 2511 (2009).

[15] Morell G, Katiyar R S and Weisz S Z, Appl. Phys. Lett. **69**, 987 (1996).

[16] Salomé P M P, Malaquias J and Fernandes P A, Solar Energy Materials & Solar Cells **101**, 147 (2012).

[17] Ganchev M, Iljina J and Kaupmees L, Thin Solid Films **519**, 7394 (2011).